Journal of Alloys and Compounds 735 (2018) 2281–2286

Contents lists available at ScienceDirect

Journal of Alloys and Compounds

journal homepage: http://www.elsevier.com/locate/jalcom

Diffusive and displacive phase transitions in Ti–Fe and Ti–Co alloys under high pressure torsion

B.B. Straumal [a, b, c, *], A.R. Kilmametov [a], Yu. Ivanisenko [a], A.A. Mazilkin [a, b], R.Z. Valiev [d], N.S. Afonikova [b], A.S. Gornakova [b], H. Hahn [a]

[a] Karlsruhe Institute of Technology (KIT), Institute of Nanotechnology, Hermann-von-Helmholtz-Platz 1, 76344, Eggenstein-Leopoldshafen, Germany
[b] Institute of Solid State Physics, Russian Academy of Sciences, Ac. Ossipyan Str. 2, 142432, Chernogolovka, Russia
[c] National University of Science and Technology «MISIS», Leninskii Prosp. 4, 119049, Moscow, Russia
[d] Saint Petersburg State University, 28 Universitetskiy Pr., Saint Petersburg, 198504, Russia

ARTICLE INFO

Article history:
Received 1 August 2017
Received in revised form
13 November 2017
Accepted 28 November 2017
Available online 29 November 2017

Keywords:
High-pressure torsion
Ti–Fe alloys
Ti–Co alloys
Decomposition of solid solution
Phase transitions

ABSTRACT

The high pressure torsion (HPT) of Ti–4 wt. % Fe and Ti–4 wt. % Co alloys has been studied. Before HPT, the samples were annealed above and below the temperature of eutectoid transformation. After quenching, the first samples contained a mixture of α and β phases. The latter samples contained a mixture of α-Ti saturated with Fe or Co and respective intermetallic phases TiFe. During HPT the high-pressure ω-phase formed in all samples. The amount of ω-phase was higher when the initial samples contained the α+β mixture then in the case of α+TiFe or α+Ti_2Co mixture. Most probably, the martensitic β→ω transformation occurs easier than the α→ω one. The amount of ω-phase was higher in Ti–Fe alloy than in the Ti–Co alloy for both initial states. It seems that cobalt additions disadvantageously change the lattice parameters in Ti for martensitic β→ω and α→ω transformations. The phase transformations with mass transfer (diffusive ones) also take place by HPT of Ti–Fe and Ti–Co alloys. Both α-based solid solutions partially decomposed after HPT. After HPT, the lattice parameters of α-phase containing cobalt or iron changed towards those of pure α-Ti. It has been observed for the first time that the composition of TiFe phase also changes after HPT.

1. Introduction

Severe plastic deformation (SPD) stands for a group of novel technologies, which allow engineers and metallurgists to control the structure and properties of materials in a new way [1]. The main feature of SPD is the possibility to deform a piece of material in a confined space. In such a way the strain can be extremely high without breaking the piece apart. If a piece cannot destroy during straining, the dynamic equilibrium should appear between production and annihilation of defects. Such a dynamic equilibrium establishes after a certain strain value. Thus, it is quite understandable that SPD leads to various phase transformations [2,3] e.g. the decomposition [4–6] or formation [7,8] of a supersaturated solid solution, disordering of ordered phases [9,10], dissolution of phases [11–15], amorphization of crystalline phases [3,16–19], appearance of the high-temperature [20], low-temperature [10,12], or high-pressure [21–23] allotropic modifications, and nanocrystallization in the amorphous matrix [24–27].

This paper is devoted to the displacive and diffusive phase transitions in Ti–Fe and Ti–Co alloys under high pressure torsion. Displacive (or diffusionless, or martensitic) are the β→ω and α→ω phase transformations. The martensitic nature of these transformations reflect itself in the special orientation relationships between β and ω as well as between α and ω phases: between β- and ω-phase $\{111\}_\beta \| (0001)_\omega; \langle 1\bar{1}0\rangle_\beta \| \langle 11\bar{2}0\rangle_\omega$ [28], between α- and ω-phases OR 1 $(0001)_\alpha \| (01\bar{1}1)_\omega; \langle 11\bar{2}0\rangle_\alpha \| \langle 1\bar{1}01\rangle_\omega$ or OR 2 $(0001)_\alpha \| (11\bar{2}0)_\omega; \langle 11\bar{2}0\rangle_\alpha \| \langle 0001\rangle_\omega$ [29].

Therefore, such transformations need only small shift of the atoms and do not require the mass transfer of atoms over long distances. However, SPD can lead also to the diffusive phase transformations like decomposition of (supersaturated) solid solution and the dissolution of precipitates. We can expect such transitions also in the Ti–Fe and Ti–Co alloys.

* Corresponding author. Institute of Solid State Physics, Russian Academy of Sciences, Ac. Ossipyan Str. 2, 142432, Chernogolovka, Russia.
E-mail addresses: straumal@issp.ac.ru, straumal@mf.mpg.de (B.B. Straumal).

https://doi.org/10.1016/j.jallcom.2017.11.317
0925-8388/

Previously, we studied the phase transformations in the Ti–Fe and Ti–Co alloys in the as-cast state or after annealing above the temperature of eutectoid phase transformation T_e, i.e. in the α+β two-phase area of respective phase diagram [30–32]. After quenching, such samples contained a mixture of α (or α′) and β phases. The high pressure torsion (HPT) led to the formation of high-pressure ω-phase. The ω-phase is metastable at ambient pressure. The goal of this work is to study the HPT-driven phase transformations in Ti–Fe and Ti–Co alloys annealed below T_e. Such alloys contain before HPT the mixture of α-phase (saturated with iron or cobalt atoms) as a matrix and particles of respective intermetallic phases.

2. Experimental

Pure titanium as well as Ti alloys with 4 wt% Fe and 4 wt% Co were investigated (3.45 at.% Fe and 3.28 at.% Co, respectively). The alloys were inductively melted in vacuum of high purity components (99.9% Ti, 99.97% Fe and 99.99% Co). The melt was poured in vacuum into the water-cooled cylindrical copper crucible of 10 mm diameter. After sawing, grinding, and chemical etching, the 0.7 mm thick disks cut from the as-cast cylinders were placed in sealed and evacuated silica ampoules (residual pressure, $p = 4 \times 10^{-4}$ Pa). They have been annealed at $T = 800$ °C, 270 h, $T = 470$ °C, 750 h (Ti–Fe alloys) and at $T = 800$ °C, 91 h, $T = 670$ °C, 168 h, $T = 600$ °C, 2774 h (Ti–Co alloys) and then quenched in water at room temperature. After annealing and quenching the samples were deformed by high-pressure torsion in a Bridgman anvil type unit (room temperature, pressure at 7 GPa, 1 rotation-per-minute, 5 rotations) using a custom built computer-controlled HPT device (W. Klement GmbH, Lang, Austria). Pure titanium was deformed in the as-cast state. The torsion torque measured during HPT increased during 1–2 anvil rotations and then remained unchanged (i.e. reached a steady state as in Refs. [4,5,8,31,33–35]). The cold working in the HPT machine leads to slight heating of a sample up to about 40–50 °C in the steady state. After HPT, the central (low-deformed) part of each disk (about 3 mm in diameter) was excluded from further investigations. The 2 mm thick slices were also cut from the ∅ 10 mm cylindrical ingots and then divided into four parts. These as-cast samples were embedded in resin and then mechanically ground and polished, using 1 μm diamond paste in the last polishing step, for the metallographic study. After etching, the as-cast samples were investigated by means of the scanning electron microscopy (SEM).

X-ray diffraction patterns were obtained using Bragg–Brentano geometry in a powder diffractometer (Philips X'Pert) with Cu-Kα radiation. Transmission electron microscopy (TEM) and high resolution TEM (HREM) observations have been made by using an aberration corrected TITAN 80–300 transmission electron microscope with specimens cut from bulk samples at a 3 mm distance from the disc center and further thinned in a Tenupol 5 electropolishing device. X-rays diffraction (XRD) spectra have been collected with a Philips X'Pert powder diffraction apparatus operating in the Bragg–Brentano theta-two theta configuration and the Cu-K_α anode. The XRD peak profiles were fitted by Pseudo-Voigt function. Lattice parameter evaluation was performed by the Fityk software [36] using a Rietveld-like whole profile refinement. Relative amount of α, β and ω phases were estimated basing on the comparison of the integrated intensities. The crystallographic texture was taken into account in this estimation.

3. Results and discussion

Fig. 1 shows the bright field TEM micrographs of Ti − 4 wt% Co alloy annealed at 600 °C, 2774 h after annealing and after subsequent HPT. The temperature of 670 °C is below the temperature $T_e = 685$ °C of eutectoid transformation for the Ti–Co system [37]. Therefore, before HPT (Fig. 1a) the α-Ti matrix contains the particles of Ti_2Co intermetallic phase. They are non-faceted and slightly elongated with diameter ~0.5–1 μm and length ~1–3 μm. After HPT (Fig. 1b) the Ti_2Co particles become very fine (~10 nm) and are almost invisible. The XRD peaks of α-Ti and Ti_2Co are strongly broadened after HPT (Fig. 2b). One can suppose that the original particles were strongly fragmented during SPD, i.e. cut into small parts by the gliding dislocations. On the other hand, one can also suppose that the original Ti_2Co particles were partly dissolved in the α-Ti matrix and then re-precipitated again (like precipitates in Cu–Co or Cu–Ag alloys [33,35]).

The samples of Ti − 4 wt% Fe alloy contain after long annealing

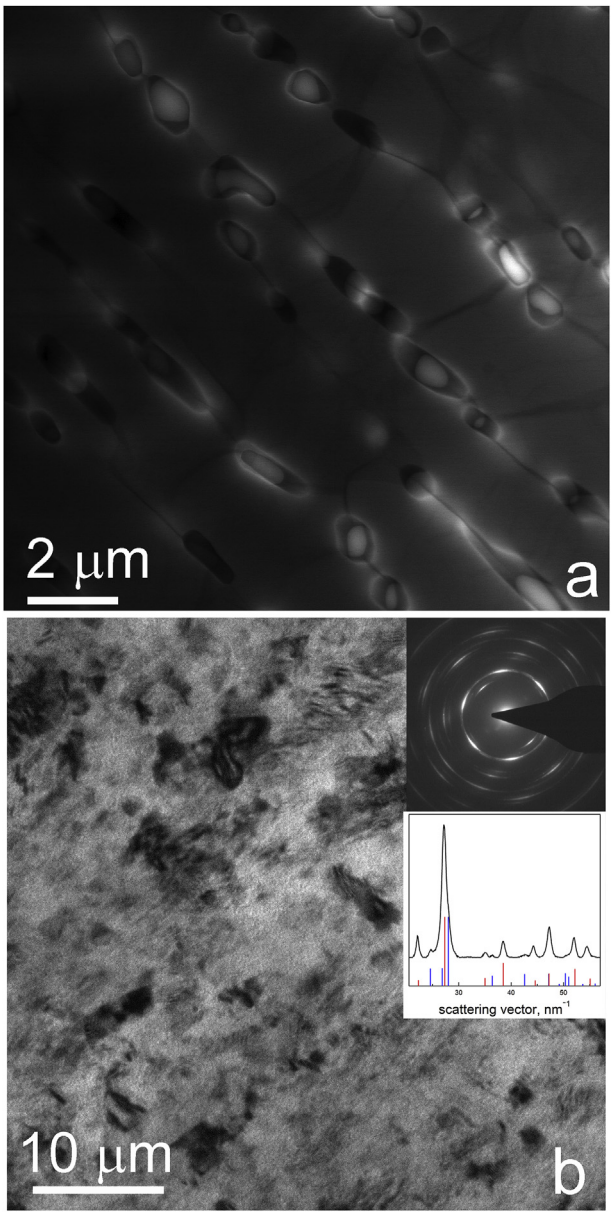

Fig. 1. Bright field TEM micrographs of Ti − 4 wt% Co alloy annealed at $T = 670$ °C, 168 h (a) after annealing before HPT and (b) after subsequent HPT. Selected area electron diffraction pattern and corresponding radial intensity distribution are shown as inserts; α and ω-Ti phases are denoted by blue and red bars correspondingly. (For interpretation of the references to colour in this figure legend, the reader is referred to the Web version of this article.)

at 470 °C, 750 h (i.e. below the temperature T_e = 596 °C for Ti–Fe system [37]) the particles of TiFe intermetallic phase with size of few μm (Fig. 2a, middle curve). After HPT the particles of TiFe become very fine of ~30 nm (Fig. 2a, upper curve). The XRD peaks of α-Ti and TiFe are strongly broadened after HPT (Fig. 2a). The phase TiFe exists in a certain concentration interval between 51.3 and 54.0 wt% Fe [37]. This circumstance is very useful for us. The precise measurements of the lattice parameter of TiFe particles show that it changes from 0.2979 nm before HPT to 0.2989 nm after HPT (see also Table 1). The comparison with published literature data on Vegard law for TiFe phase [38–42] allows us to estimate the composition change. Thus, the intermetallic particles contain approx. 54 wt% Fe before HPT and approx. 52 wt% Fe after HPT.

At the same time, processing conditions of the HPT-technique may cause residual macrostress and consequently affect lattice parameter measurements. In our case the XRD measurements of lattice parameters of Ti–Co and Ti–Fe alloys reveal the changes of the order of magnitude of 0.0005–0.001 nm (see Table 1). The precise synchrotron measurements of residual macro-stress influence gave the possible effect of 0.00008 nm [43]. Earlier, the absence of the residual macrostress was reported for HPT samples [44]. The authors [44] checked the meanings of XRD peak shift after different times of electrolysis erosion. At present work Fig. 2 demonstrates that the noted deviations in lattice parameter do not influence the observed general trend.

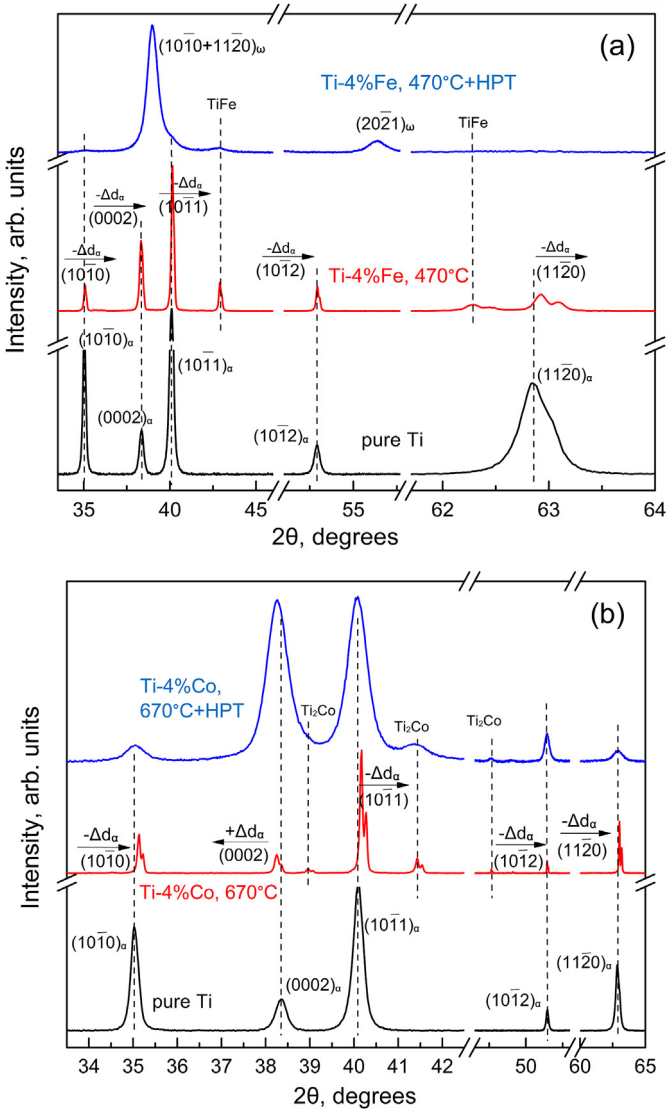

Fig. 2. XRD patterns for (a) pure titanium and Ti – 4 wt% Fe alloy annealed at 470 °C, 750 h after annealing and after subsequent HPT, (b) pure titanium and Ti – 4 wt% Co annealed at 670 °C, 168 h after annealing and after subsequent HPT.

In Fig. 2 the XRD patterns are shown for (a) pure titanium and Ti – 4 wt% Fe alloy annealed at 470 °C, 750 h before and after HPT as well as for (b) pure titanium and Ti – 4 wt% Co annealed at 670 °C, 168 h before and after HPT. These XRD data demonstrate that after long annealing below eutectoid temperature T_e the α-Ti is saturated with iron and cobalt, respectively. The lattice parameters after annealing are a = 0.29511 nm and c = 0.46940 nm in Ti – 4 wt% Fe alloy and a = 0.29481 nm and c = 0.47028 nm in Ti – 4 wt% Co alloy (Table 1). It is very good visible that after HPT the peaks of α-based solid solutions with Fe and Co move back towards the peaks of pure Ti. The lattice parameters after additional HPT treatment are a = 0.2955 nm and c = 0.4692 nm in Ti – 4 wt% Fe alloy and a = 0.2957 nm and c = 0.4703 nm in Ti – 4 wt% Co alloy. In pure titanium a = 0.2959 nm and c = 0.4690 nm (Table 1). It means that after HPT the lattice parameters a and c in Ti–Fe and Ti–Co alloys became closer to those of pure titanium. In other words, after annealing and quenching samples contained the α-Ti-based solid solution were supersaturated with Fe or Co at the room temperature (RT). HPT at RT leads to partial decomposition of this supersaturated solid solution. The α-Ti-based solid solution is purified in both cases but not completely. The lattice parameters c and a after HPT did not reach their values for pure α-Ti. It means that after HPT the α-Ti contains as much Fe or Co as if we would have been annealed it at a certain effective temperature T_{eff} between T_e and RT. This phenomenon is very similar to the HPT-driven decomposition of a supersaturated solid solution in several Cu-based alloys [39]. In Cu–Ag and Cu–Co alloys T_{eff} is a function of HPT conditions, and does not depend on the initial state of the alloy. It is, therefore, equifinal [45]. On the other hand, T_{eff} depends on the alloying element in Cu-based alloys. T_{eff} increases with increasing activation enthalpy of a second component [46]. If an alloy was annealed before HPT above T_{eff}, the solid solution decomposes, but if it was annealed before HPT below T_{eff}, the concentration in solid solution increases on the cost of partial dissolution of precipitates of a second phase (Co and Ag, respectively). The observed features of the phase transformations under HPT support the concept proposed in Refs. [47,48] about the appearance of additional channels for the dissipation of mechanical energy supplied to the solid state during SPD.

Similar to our earlier experiments [30–32], the HPT of the Ti–Fe and Ti–Co alloys annealed below T_e also leads to the formation of ω-phase. Previously, we annealed the samples in the α+β two-phase area of respective phase diagram. After quenching, such samples contained the mixture of α (or α′) and β phases. The HPT led to the formation of ω-phase. Minor amounts of α and β phases remained after HPT as well. In Fig. 3 the XRD patterns are shown for (a) Ti – 4 wt% Fe alloy annealed at 470 °C, 750 h and at 800 °C, 270 h after HPT, (b) Ti – 4 wt% Co annealed at 670 °C, 168 h and at 800 °C, 91 h after HPT. The Ti – 4 wt% Fe alloy annealed at 800 °C contains after HPT about 95% of ω-phase. The same alloy annealed at 470 °C contains after HPT only ~80% of ω-phase. The Ti – 4 wt% Co alloy annealed at 800 °C contains after HPT about 80% of ω-phase. However, the same alloy annealed at 670 °C contains no ω-phase. Thus, the percentage of ω-phase after HPT was much lower or substantially suppressed in the samples annealed below T_e than in the same alloys annealed at the high temperature in the α+β area of the phase diagram. One possible explanation for this fact is that the alloys after "low" annealing contain no β-phase, and β-phase transforms into ω-phase much easier than α-Ti. However, another explanation of these facts is also possible. We observed recently

Table 1
Lattice parameters before and after HPT.

Alloy	State	Parameter *a*, nm	Parameter *c*, nm	Intermetallic compound	Parameter *a*, nm
Ti–Fe	Before HPT	0.2951	0.4694	TiFe	0.2979
	After HPT	0.2955	0.4692	(*Pm3m*)	0.2989
Ti–Co	Before HPT	0.2948	0.4703	Ti_2Co	1.1316
	After HPT	0.2957	0.4703	(*Fd3m*)	1.1327
Pure Ti	Before HPT	0.2955	0.4694		
	After HPT	0.2959	0.4690		

that the ω-phase with a certain amount of Fe (about 4 at. % Fe [32]) is formed during HPT at easiest. It is because the addition of iron decreases the lattice parameter of β-phase, and the lattice parameter of ω-phase remains almost constant. As a result the orientation relationship needed for the diffusionless (martensitic) β-to-ω transformation fulfils optimally at about 4 at. % Fe [32]. We can suppose that the α-Ti in the samples after "low" annealing contains far too few Fe or Co, and the rest of Fe or Co atoms are scavenged in the hard intermetallic precipitates.

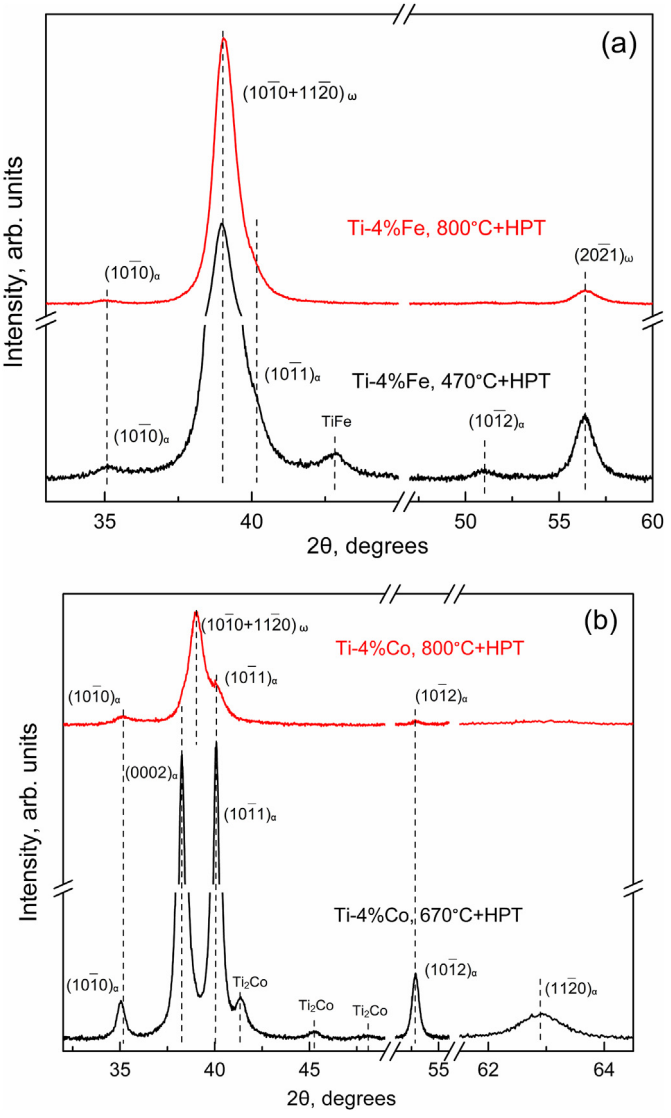

Fig. 3. XRD patterns for (a) Ti – 4 wt% Fe alloy annealed at 470 °C, 750 h and at 800 °C, 270 h after HPT, (b) Ti – 4 wt% Co annealed at 670 °C, 168 h and at 800 °C, 91 h after HPT.

Another interesting fact is that after HPT the amount of ω-phase is much less in the Ti–Co alloys in comparison with Ti–Fe alloys for similar initial states. (In our work the Ti–Fe and Ti–Co alloys contain 4 wt% of Co and Fe. The respective atomic concentration of second components are slightly different, namely 3.45 at.% Fe and 3.28 at.% Co. However, this minor difference does not change qualitatively the following conclusions.) Fig. 4 shows that HPT of the (α+β) phase mixture leads to almost complete ω-phase formation in Ti-Fe alloy (800 °C, 270 h) but to noticeable amount of remained α-phase in the Ti–Co alloy (800 °C, 91 h). However, in the case of (α + intermetallic) mixture the transformation into ω-phase appeared to be suppressed in the Ti-Co alloy (Fig. 2b). One of the possible reasons could be the different influence of alloying with Fe and Co on the α-Ti lattice. Thus, the addition of cobalt increases the *c/a* ratio for the hexagonal closely-packed lattice of α-Ti. This ratio comes closer to the ideal value of $c/a = 1.63$ for closely packed spheres. This *c/a* value maybe less convenient for the orientation relationships needed for the diffusionless α-to-ω transition.

4. Conclusions

Severe plastic deformation not only leads to the grain refinement but also drives the phase transformations in materials. The high pressure torsion of Ti–4 wt. % Fe and Ti–4 wt. % Co alloys has been studied for two initial states: (1) mixture of α and β phases and (2) mixture of α-phase and intermetallic compounds TiFe, $TiFe_2$ or Ti_2Co. HPT leads to martensitic β→ω and α→ω transformations. The martensitic β→ω transformation occurs easier than the α→ω one. Thus, the amount of ω-phase was observed to be higher when the initial samples contained the α+β mixture then in the case of

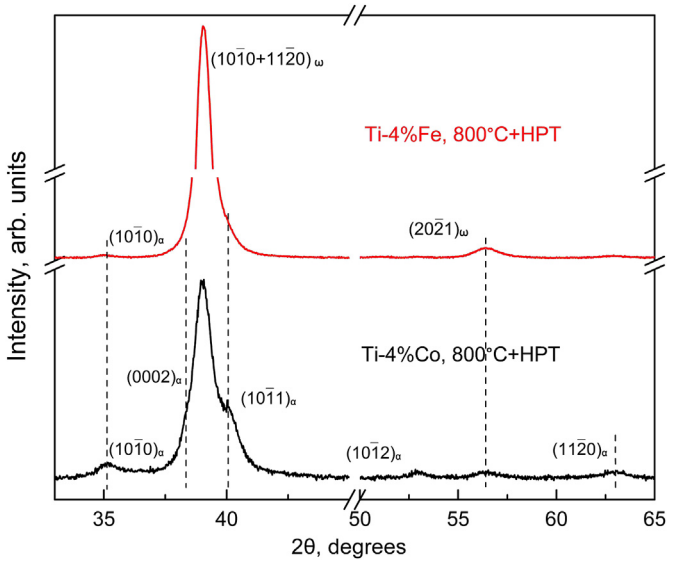

Fig. 4. XRD patterns for Ti – 4 wt% Fe and Ti – 4 wt% Co alloys annealed at 800 °C after HPT.

α+ (TiFe, $TiFe_2$) or α+ Ti_2Co mixture. The amount of ω-phase was higher in Ti–Fe alloys than in the Ti–Co alloys for both initial states. Most probably, it is because cobalt additions disadvantageously change the lattice parameters in Ti for martensitic β→ω and α→ω transformations. The α-based solid solutions with Fe and Co partially decomposed after HPT. Thus, the diffusive phase transformations with mass transfer also took place during HPT. The iron concentration in TiFe phase slightly changed after HPT as well. Most probably, the TiFe particles were not simply fragmented by cutting during HPT but completely dissolved in the α-matrix and then re-precipitated.

Acknowledgements

We would like to thank Prof. D.R. Trinkle for fruitful discussion. The work was partially supported by Deutsche Forschungsgemeinschaft (project numbers IV 98/5-1, HA 1344/32-1), Russian Foundation for Basic Research (grant 16-53-12007 and 16-03-00285), Ministry of Education and Science of the Russian Federation in the framework of the Program to Increase the Competitiveness of NUST "MISiS", and Karlsruhe Nano Micro Facility. One of the authors (RZV) acknowledges the Saint-Petersburg State University for research grant No. 6.65.43.2017.

References

[1] R.Z. Valiev, R.K. Islamgaliev, I.V. Alexandrov, Bulk nanostructured materials from severe plastic deformation, Progr. Mater. Sci. 45 (2000) 103–189.
[2] X. Sauvage, A. Chbihi, X. Quelennec, Severe plastic deformation and phase transformations, J. Phys. 240 (2010), 012003.
[3] B. Straumal, A. Korneva, P. Zięba, Phase transitions in metallic alloys driven by the high pressure torsion, Arch. Civil Mech. Eng. 14 (2014) 242–249.
[4] B.B. Straumal, S.G. Protasova, A.A. Mazilkin, E. Rabkin, D. Goll, G. Schütz, B. Baretzky, R.Z. Valiev, Deformation-driven formation of equilibrium phases in the Cu–Ni alloys, J. Mater. Sci. 47 (2012) 360–367.
[5] A.A. Mazilkin, B.B. Straumal, E. Rabkin, B. Baretzky, S. Enders, S.G. Protasova, O.A. Kogtenkova, R.Z. Valiev, Softening of nanostructured Al–Zn and Al–Mg alloys after severe plastic deformation, Acta Mater. 54 (2006) 3933–3939.
[6] B.B. Straumal, B. Baretzky, A.A. Mazilkin, F. Phillipp, O.A. Kogtenkova, M.N. Volkov, R.Z. Valiev, Formation of nanograined structure and decomposition of supersaturated solid solution during high pressure torsion of Al–Zn and Al–Mg, Acta Mater. 52 (2004) 4469–4478.
[7] W. Lojkowski, M. Djahanbakhsh, G. Burkle, S. Gierlotka, W. Zielinski, H.J. Fecht, Nanostructure formation on the surface of railway tracks, Mater. Sci. Eng. A 303 (2001) 197–208.
[8] X. Sauvage, X. Quelennec, J.J. Malandain, P. Pareige, Nanostructure of a cold drawn tempered martensitic steel, Scripta Mater. 54 (2006) 1099–1103.
[9] V.V. Sagaradze, V.A. Shabashov, Deformation-induced anomalous phase transformations in nanocrystalline FCC Fe–Ni based alloys, Nanostruct. Mater. 9 (1997) 681–684.
[10] B.B. Straumal, A.A. Mazilkin, S.G. Protasova, S.V. Dobatkin, A.O. Rodin, B. Baretzky, D. Goll, G. Schütz, Fe–C nanograined alloys obtained by high pressure torsion: structure and magnetic properties, Mater. Sci. Eng. A 503 (2009) 185–189.
[11] A.V. Korznikov, G. Tram, O. Dimitrov, G.F. Korznikova, S.R. Idrisova, Z. Pakiela, The mechanism of nanocrystalline structure formation in Ni_3Al during severe plastic deformation, Acta Mater. 49 (2001) 663–671.
[12] B.B. Straumal, S.V. Dobatkin, A.O. Rodin, S.G. Protasova, A.A. Mazilkin, D. Goll, B. Baretzky, Structure and properties of nanograined Fe–C alloys after severe plastic deformation, Adv. Eng. Mater. 13 (2011) 463–469.
[13] C. Rentenberger, H.P. Karnthaler, Extensive disordering in long-range-ordered Cu_3Au induced by severe plastic deformation studied by transmission electron microscopy, Acta Mater. 56 (2008) 2526–2530.
[14] Y. Ivanisenko, I. MacLaren, X. Sauvage, R.Z. Valiev, H.-J. Fecht, Shear-induced α → γ transformation in nanoscale Fe–C composite, Acta Mater. 54 (2006) 1659–1669.
[15] C.M. Cepeda-Jiménez, J.M. García-Infanta, A.P. Zhilyaev, O.A. Ruano, F. Carreño, Influence of the thermal treatment on the deformation-induced precipitation of a hypoeutectic Al–7 wt% Si casting alloy deformed by high-pressure torsion, J. Alloys Compd. 509 (2011) 636–643.
[16] A.A. Mazilkin, G.E. Abrosimova, S.G. Protasova, B.B. Straumal, G. Schütz, S.V. Dobatkin, A.S. Bakai, Transmission electron microscopy investigation of boundaries between amorphous "grains" in $Ni_{50}Nb_{20}Y_{30}$ alloy, J. Mater. Sci. 46 (2011) 4336–4342.
[17] S.D. Prokoshkin, I.Yu. Khmelevskaya, S.V. Dobatkin, I.B. Trubitsyna, E.V. Tatyanin, V.V. Stolyarov, E.A. Prokofiev, Alloy composition, deformation temperature, pressure and post-deformation annealing effects in severely deformed Ti–Ni based shape memory alloys, Acta Mater. 53 (2005) 2703–2714.
[18] B.B. Straumal, A.A. Mazilkin, S.G. Protasova, D.V. Gunderov, G.A. López, B. Baretzky, Amorphization of crystalline phases in the Nd-Fe-B alloy driven by the high-pressure torsion, Mater. Lett. 161 (2015) 735–739.
[19] V.V. Stolyarov, D.V. Gunderov, A.G. Popov, V.S. Gaviko, A.S. Ermolenko, Structure evolution and changes in magnetic properties of severe plastic deformed Nd(Pr)–Fe–B alloys during annealing, J. Alloys Compd. 281 (1998) 69–71.
[20] Y. Ivanisenko, I. MacLaren, X. Sauvage, R.Z. Valiev, H.J. Fecht, Shear-induced α → γ transformation in nanoscale Fe–C composite, Acta Mater. 54 (2006) 1659–1669.
[21] B.B. Straumal, A.R. Kilmametov, Yu. Ivanisenko, A.S. Gornakova, A.A. Mazilkin, M.J. Kriegel, O.B. Fabrichnaya, B. Baretzky, H. Hahn, Phase transformations in Ti-Fe alloys induced by high pressure torsion, Adv. Eng. Mater. 17 (2015) 1835–1841.
[22] K. Edalati, Z. Horita, Y. Mine, High-pressure torsion of hafniurn, Mater. Sci. Eng. A 527 (2010) 2136–2141.
[23] M.T. Pérez-Prado, A.P. Zhilyaev, First experimental observation of shear induced hcp to bcc transformation in pure Zr, Phys. Rev. Lett. 102 (2009), 175504.
[24] Zs. Kovács, P. Henits, A.P. Zhilyaev, N.Q. Chinh, Á. Révész, Microstructural characterization of the crystallization sequence of a severe plastically deformed Al-Ce-Ni-Co amorphous alloy, Mater. Sci. Forum 519–521 (2006) 1329–1334.
[25] G.E. Abrosimova, A.S. Aronin, S.V. Dobatkin, S.D. Kaloshkin, D.V. Matveev, O.G. Rybchenko, E.V. Tatyanin, I.I. Zverkova, The formation of nanocrystalline structure in amorphous Fe-Si-B alloy by severe plastic deformation, J. Metastab. Nanocryst. Mater. 24 (2005) 69–72.
[26] A.M. Glezer, M.R. Plotnikova, A.V. Shalimova, S.V. Dobatkin, Severe plastic deformation of amorphous alloys: I. Structure and mechanical properties, Bull. Russ. Ac. Sci. Phys. 73 (2009) 1233–1236.
[27] S. Hóbor, Á. Révész, A.P. Zhilyaev, Zs. Kovácz, Different nanocrystallization sequence during high pressure torsion and thermal treatments of amorphous $Cu_{60}Zr_{20}Ti_{20}$ alloy, Rev. Adv. Mater. Sci. 18 (2008) 590–592.
[28] B.S. Hickman, The Formation of omega phase in Ti and Zr alloys: a review, J. Mater. Sci. 4 (1969) 554–563.
[29] D.R. Trinkle, R.G. Hennig, S.G. Srinivasan, D.M. Hatch, M.D. Jones, H.T. Stokes, R.C. Albers, J.W. Wilkins, New mechanism for the alpha to omega martensitic transformation in pure titanium, Phys. Rev. Lett. 91 (2003), 025701.
[30] A. Kilmametov, Yu. Ivanisenko, B. Straumal, A.A. Mazilkin, A.S. Gornakova, M.J. Kriegel, O.B. Fabrichnaya, D. Rafaja, H. Hahn, Transformations of α' martensite in Ti–Fe alloys under high pressure torsion, Scripta Mater. 136 (2017) 46–49.
[31] B.B. Straumal, A.R. Kilmametov, Yu. Ivanisenko, A.S. Gornakova, A.A. Mazilkin, M.J. Kriegel, O.B. Fabrichnaya, B. Baretzky, H. Hahn, Phase transformations in Ti-Fe alloys induced by high pressure torsion, Adv. Eng. Mater. 17 (2015) 1835–1841.
[32] A.R. Kilmametov, Yu. Ivanisenko, A.A. Mazilkin, B.B. Straumal, A.S. Gornakova, O.B. Fabrichnaya, M.J. Kriegel, D. Rafaja, H. Hahn, The α→ω and β→ω phase transformations in Ti–Fe alloys under high-pressure torsion, Acta Mater. (2018), https://doi.org/10.1016/j.actamat.2017.10.051.
[33] B.B. Straumal, A.R. Kilmametov, Yu.O. Kucheev, L. Kurmanaeva, Yu. Ivanisenko, B. Baretzky, A. Korneva, P. Zięba, D.A. Molodov, Phase transitions during high pressure torsion of Cu–Co alloys, Mater. Lett. 118 (2014) 111–114.
[34] B. Straumal, R. Valiev, O. Kogtenkova, P. Zieba, T. Czeppe, E. Bielanska, M. Faryna, Thermal evolution and grain boundary phase transformations in severe deformed nanograined Al–Zn alloys, Acta Mater. 56 (2008) 6123–6131.
[35] B.B. Straumal, V. Pontikis, A.R. Kilmametov, A.A. Mazilkin, S.V. Dobatkin, B. Baretzky, Competition between precipitation and dissolution in Cu–Ag alloys under high pressure torsion, Acta Mater. 122 (2017) 60–71.
[36] M. Wojdyr, Fityk: a general-purpose peak fitting program, J. Appl. Cryst. 43 (2010) 1126–1128.
[37] T.B. Massalski (Ed.), Binary Alloy Phase Diagrams, second ed., ASM International, Materials Park, OH, 1990.
[38] Y. Murakami, H. Kimura, Y. Nishimura, An investigation on the titanium-iron-carbon system, Trans. Nat. Res. Inst. Met. Jpn. 1 (1) (1959) 7–21.
[39] H.P. Stüwe, Y. Shimomura, Lattice constants of cubic phases FeTi, CoTi, NiTi, Z. Metallkunde 3 (1960) 180–181.
[40] R. Ray, B.C. Giessen, N.J. Grant, The constitution of metastable titanium-rich Ti–Fe alloys: an order-disorder transition, Metall. Trans. 3 (1972) 627–629.
[41] K. Ikeda, Kondo effect in the transport properties of the CsCl-type compounds $Fe_{1-x}Ti_{1+x}$: II. Magnetic scattering center due to atomic disordering, Phys. Stat. Sol. B 63 (1974) 361–370.
[42] D. Dew-Hughes, The addition of Mn and Al to the hydriding compound FeTi: range of homogeneity and lattice parameters, Metal. Trans. A 11 (1980) 1219–1225.
[43] L. Kurmanaeva, Y. Ivanisenko, J. Markmann, Grain refinement and mechanical properties in ultrafine-grained Pd and Pd–Ag alloys produced by HPT, Mater. Sci. Eng. A 527 (2010) 1776–1783.
[44] K. Zhang, I.V. Alexandrov, R.Z. Valiev, K. Lu, Structural characterization of nanocrystalline copper by means of X-ray diffraction, J. Appl. Phys. 80 (1996) 5617–5624.
[45] L. von Bertalanffy, General system theory: a new approach to unity of science,

Human Biol. 23 (1951) 302–312.
[46] B.B. Straumal, A.R. Kilmametov, A. Korneva, A.A. Mazilkin, P.B. Straumal, P. Zięba, B. Baretzky, Phase transitions in Cu-based alloys under high pressure torsion, J. Alloys Compd. 707 (2017) 20–26.
[47] R.A. Andrievski, A.M. Glezer, Strength of nanostructures, Phys. Usp. 52 (2009) 315–344.
[48] A.M. Glezer, R.V. Sundeev, General view of severe plastic deformation in solid state, Mater. Lett. 139 (2015) 455–457.